

Noise-induced quenched disorder in dense active systems

Guozheng Lin,^{1,*} Zhangang Han,^{1,†} Amir Shee,^{2,‡} and Cristián Huepe^{1,2,3,§}

¹*School of Systems Science, Beijing Normal University, Beijing, People's Republic of China*

²*Northwestern Institute on Complex Systems and ESAM,*

Northwestern University, Evanston, IL 60208, United States of America

³*CHuepe Labs, 2713 West Haddon Ave #1, Chicago, IL 60622, United States of America*

(Dated: April 10, 2023)

We report and characterize the emergence of a noise-induced state of quenched disorder in a generic model describing a dense sheet of active polar disks with non-isotropic rotational and translational dynamics. In this state, randomly oriented self-propelled disks become jammed, only displaying small fluctuations about their mean positions and headings. The quenched disorder phase appears at intermediate noise levels, between the two states that typically define the flocking transition (a standard disordered state that displays continuously changing headings due to rotational diffusion and a polar order state of collective motion). We find that the angular fluctuations in this dense system follow an Ornstein-Uhlenbeck process leading to retrograde forces that oppose self-propulsion, and determine its properties. Using this result, we explain the mechanism behind the emergence of the quenched state and compute analytically its critical noise, showing that it matches our numerical simulations. We argue that this novel type of state could be observed in a broad range of natural and artificial dense active systems with repulsive interactions.

Active agents convert stored or ambient energy into mechanical work, injecting it at the smallest scales of the system [1–3]. They typically introduce activity through some form of self-propulsion, interact with neighbors via alignment or attraction-repulsion forces, and can be affected by noise. Many different models of active systems have been studied in recent years, with multiple parameter combinations, which could have potentially resulted in a variety of regimes and nonequilibrium phases. Only a few have been identified up to now, however, corresponding to self-organized states with various forms of (polar or nematic) orientational order [4–6], clustering [7, 8], or phase separation [9, 10]; as well as to disordered states where agents move in randomly changing directions.

One of the most studied phases displaying orientational order is characterized by collective motion, a state in which all agents are aligned and head in a common direction [11, 12]. Examples of collective motion can be found in different types of biological systems, including cytoskeleton-motor proteins [13–15], bacterial colonies [16–18], insect swarms [19, 20], bird flocks [21, 22], and fish schools [23–25]. It can also develop in artificial systems, such as active colloidal suspensions [7], colloidal rollers [26, 27], vibrated polar disks [28, 29], or robot swarms [30–37]. This type of self-organization was originally thought to require local alignment interactions [38], but has recently been shown to also emerge from a local coupling between attraction-repulsion forces and heading directions [39]. Regardless of the underlying mechanism, collective motion corresponds in all these cases to an ordered phase of aligned agents that emerges from a disordered phase with randomly changing headings. Additionally, both phases are sometimes subdivided into parameter regions with different density distributions [8, 10, 40–47].

Beyond collective motion, other collective states have been identified more recently in elastic or jammed active solids [48–50]. In these systems, attraction-repulsion forces or steric interactions between densely packed agents can result in different forms of collective oscillations and disordered dynamics [50, 51]. Despite some initial studies, very little is known about the spatiotemporal states that can develop in active solids or active jamming [51, 52].

In this Letter, we report the emergence of a noise-induced state of *quenched disorder* (QD) in densely packed active systems, where agents become jammed and their headings fluctuate about different fixed random directions. This QD phase appears at intermediate noise levels: For lower noise, most systems self-organize into a state of collective motion that we will refer to as moving order (MO); for higher noise, they reach a standard state of dynamic disorder (DD) where all heading are randomly changing. We characterize the QD phase in a generic, minimal model of self-propelled disks with off-centered rotation and linear repulsive interactions. These are similar to the active polar disks with steric interactions introduced in [28, 29], but with soft repulsive cores and non-isotropic damping. Using this model, we identify the mechanism that leads to QD, describe it analytically, and show that it could develop in a broad range of systems.

We consider a system of self-propelled polar disks with rotation axes located behind their geometric centers, interacting through linear repulsive forces. These can be viewed as minimal representations of self-propelled agents that are nonaxisymmetric about their centers of rotation and thus interact with neighbors anisotropically, which introduces torques. Figure 1(a) illustrates the interactions between two such disks, i and j , with radii

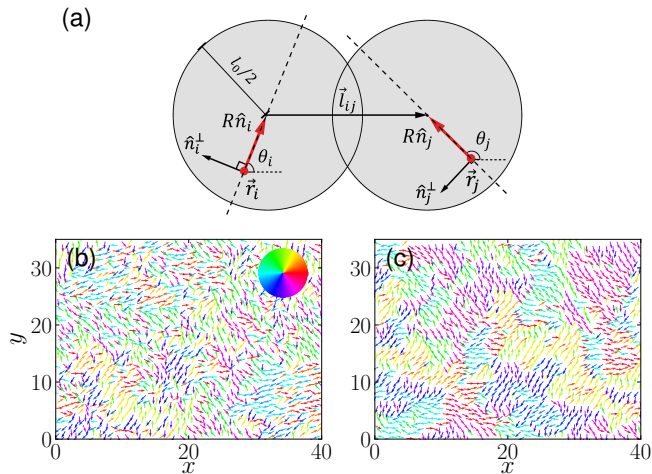


FIG. 1. (Color online) Schematic representation of model interactions and snapshots of quenched disorder states. Top: Diagram of two soft disks (a), with repulsion radius $l_0/2$ and self-propelled headings, \hat{n}_i and \hat{n}_j , translate and rotate about their axes, \vec{r}_i and \vec{r}_j , located a distance R behind each centroid. The linear repulsion, proportional to disk overlap $\|\vec{l}_{ij}\| - l_0$, is projected onto each centroid, resulting in forces and torques about \vec{r}_i and \vec{r}_j . Bottom: Typical quenched disorder state obtained from random initial conditions (b) and a fully aligned initial state (c), both placed on a periodic arena, initially forming a perfect hexagonal lattice. Each disk is represented by an arrow that starts at its centroid, points in its heading direction, and is colored by angle (see inset).

$l_0/2$ and heading directions \hat{n}_i and \hat{n}_j . Their axes of rotation \vec{r}_i and \vec{r}_j are positioned at a distance $0 \leq R \leq l_0/2$ behind their centroids, so R controls the degree of eccentricity of their rotational motion. This implies that, for small R , the interaction forces will mainly affect disk positions, whereas for large R , they will mainly affect their orientations.

We define the interaction between two neighboring disks, i and j , as a linear repulsive central force, given by $\vec{f}_{ij} = k(|\vec{l}_{ij}| - l_0)\vec{l}_{ij}/|\vec{l}_{ij}|$ if $|\vec{l}_{ij}| \leq l_0$, and by $\vec{f}_{ij} = 0$ otherwise. Here, k determines the repulsion strength and \vec{r}_{ij} is the vector that joins both geometric centers, which can be expressed in terms of the positions of the axes of rotation and the headings as $\vec{l}_{ij} = (\vec{r}_j - \vec{r}_i) + R(\hat{n}_j - \hat{n}_i)$. The total force over disk i is thus given by the sum of pairwise interactions $\vec{F}_i = \sum_j \vec{f}_{ij}$, where $j \in S_i$ is the set of all disks that overlap i (i.e., with center-to-center distance smaller than l_0). Note that, if we add linear attraction forces between neighbors for $|\vec{l}_{ij}| > l_0$, this model would describe the active elastic sheet presented in [48], formed by an hexagonal array of self-propelled rods with front tips permanently linked by linear springs.

By decomposing the effect of the total interactions \vec{F}_i over the centroid of each disk i into displacement forces and torques about its axis of rotation, we find the follow-

ing overdamped dynamical equations

$$\dot{\vec{r}}_i = v_0 \hat{n}_i + \hat{n}_i \hat{n}_i^T \left(\alpha_{\parallel} \vec{F}_i + \sqrt{2D_{\parallel}} \vec{\zeta}_i \right) + (\mathbb{I} - \hat{n}_i \hat{n}_i^T) \left(\alpha_{\perp} \vec{F}_i + \sqrt{2D_{\perp}} \vec{\zeta}_i \right), \quad (1)$$

$$\dot{\hat{n}}_i = \beta (\mathbb{I} - \hat{n}_i \hat{n}_i^T) \vec{F}_i + \sqrt{2D_{\theta}} \eta_i(t) \hat{n}_i^{\perp}. \quad (2)$$

Here, v_0 is the self-propulsion speed and \hat{n}_i^{\perp} is a unit vector perpendicular to \hat{n}_i . Note that, in order to consider a more general model, we included above the possibility of having different damping and noise levels for the disk rotation, front-back translation (along \hat{n}_i), and side-ways translation (along \hat{n}_i^{\perp}). Rotational motion is thus controlled in Eq. (2) by the inverse rotational damping coefficient β and angular diffusion constant D_{θ} , whereas translation is controlled in Eq. (1) by damping coefficients α_{\parallel} , α_{\perp} and diffusion constants D_{\parallel} , D_{\perp} (along \hat{n}_i , \hat{n}_i^{\perp} , respectively) [32, 48]. Angular noise is introduced through a delta-correlated Gaussian random variable $\eta_i(t)$, with $\langle \eta_i \rangle = 0$ and $\langle \eta_i(t) \eta_j(t') \rangle = \delta_{ij} \delta(t - t')$. Positional noise, through a vectorial delta-correlated random variable $\vec{\zeta}_i(t)$, composed of two independent Gaussian random variables $\zeta_i^x(t)$ and $\zeta_i^y(t)$, where $\langle \vec{\zeta}_i \rangle = 0$ and $\langle \zeta_i^k(t) \zeta_j^l(t') \rangle = \delta_{ij} \delta_{kl} \delta(t - t')$, with indexes k and l representing x or y .

We carried out simulations of N self-propelled polar disks, using Euler's method to integrate Eqs. (1) and (2) synchronously for all disks in a periodic rectangular arena of size $l_0 \sqrt{N} \times l_0 \sqrt{3N}/2$. For N even, this fits exactly $\sqrt{N} \times \sqrt{N}$ disks in a perfect hexagonal lattice with all neighbors at the edge of their repulsive potentials (i.e., with distance l_0 between neighboring geometrical centers). This spatial configuration was used as initial condition, with all angles either aligned in the x direction or selected at random. As we explored the phase space, we found three possible steady states: MO, DD, and the aforementioned QD state. States MO and DD have been well documented in the literature, as they correspond to the standard order-disorder (flocking) transition in collective motion. Instead, state QD had not been previously reported and will be the focus of what remains of this Letter.

Figures 1(b) and 1(c) display examples of QD states obtained in simulations. Panel (b) is a snapshot of the stationary solution reached starting from random initial angles, whereas panel (c) shows the state reached starting with all headings aligned. We observe that the final spatial distribution depends on the initial conditions, as the latter presents larger domains of locally aligned agents. In both cases, all disks are jammed when the QD state is reached, presenting essentially fixed mean positions and orientations. Note, however, that some changes may occur due to particle rearrangements, especially in smaller systems, but these will only develop at extremely large timescales.

Our phase space explorations found that QD appears for various combinations of the parameters in Eqs. (1) and (2), as we show in the Supplemental Material [53], but not in the often studied case with fully isotropic damping ($\alpha_{\parallel} = \alpha_{\perp}$), or in limit cases with no angular noise ($D_{\theta} = 0$) or no rotational anisotropy ($R = 0$). In order to study the emergence of QD in the simplest possible context, we will thus focus on a different limit case, setting $\alpha_{\perp} = D_{\parallel} = D_{\perp} = 0$, with $\alpha_{\parallel} > 0$ and $D_{\theta} > 0$. In addition, we will fix in all simulations below $\alpha_{\parallel} = 0.02$, $\beta = 1.2$, $k = 5$, $l_0 = 1$, $v_0 = 0.002$, $N = 1600$, and $dt = 0.01$, while varying R , D_{θ} .

To analyze our simulation results, we introduce two order parameters that allow us to discriminate between the collective states. The first one corresponds to the standard polarization $\psi = \langle \|\sum_{i=1}^N \hat{n}_i\| \rangle_t / N$ (where $\langle \cdot \rangle_t$ is the average over time after reaching a steady state), which determines the degree of alignment between agents. We thus have $\psi = 1$ if all agents are perfectly aligned and $\psi = 0$ if they are randomly oriented. The second one evaluates the persistence of the orientation of each agent over time, averaged over all agents, and is defined by $\phi = \sum_{i=1}^N \|\langle \hat{n}_i \rangle_t\| / N$. If the orientation of each agent fluctuates about a fixed mean value, we have $\phi = 1$; if they are randomly rotating over time, $\phi = 0$.

Figure 2 presents the three phases obtained in our simulations, as a function either of D_{θ} for fixed $R = 0.3$ (a,b), or of R for fixed $D_{\theta} = 0.2$ (c,d). Panels (a) and (c) show the steady state values of ψ (o) and ϕ (◊), starting from either aligned (open symbols) or random (solid symbols) headings. Panel (a) shows that we find the MO phase ($\psi \approx \phi \approx 1$) at low D_{θ} , with agents displaying long-range polar order and a persistent orientation. At high D_{θ} , for either low or high R values, we find the DD phase ($\psi \approx \phi \approx 0$), where headings are continuously randomly changing in any direction. Finally, at intermediate D_{θ} and R values, we find the QD phase ($\psi \approx 0$ and $\phi \approx 1$), where each agent has a (randomly oriented) constant mean heading, about which its instantaneous orientation is fluctuating.

To help identify the boundaries between the phases, we compute in Figs. 2(b,d) the order parameter variances, labeled ψ_2 and ϕ_2 . Their maxima correspond to the transition points used to color the MO, DD, and QD regions in panels (a) and (c). Panel (a) shows that the QD phase is only found at intermediate noise levels for $R = 0.3$, between the MO and DD phases. Panel (d) shows that it also requires intermediate R values; if R is too big or too small, the system falls into the DD phase. Note that the transition between MO and DD occurs at a slightly lower critical D_{θ} when simulations are started from a state with random, rather than aligned, headings.

We now describe the mechanism that leads to the QD state and postulate an approximate representation of its dynamics that will allow us to describe it analytically. We begin by noting that, in a densely packed system and

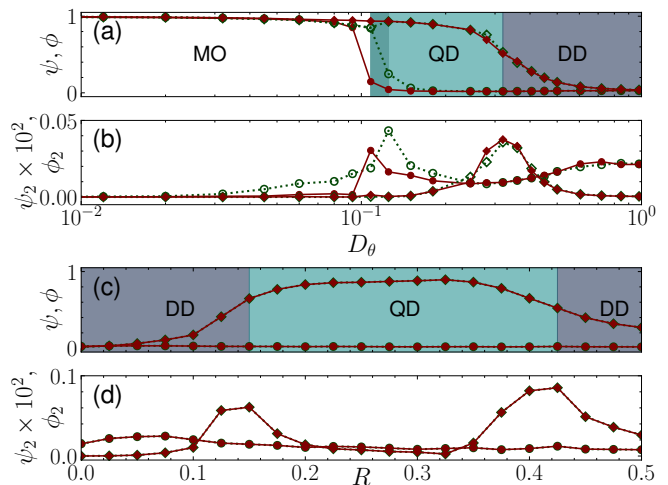


FIG. 2. (Color online) Order parameters (a,c) and their variances (b,d) as a function of angular noise D_{θ} (a,b) and degree of rotational eccentricity R (c,d), for fixed $R = 0.3$ or fixed $D_{\theta} = 0.2$, respectively. The standard polarization order parameter ψ (o) and orientation persistence order parameter ϕ (◊) are presented, using solid or open symbols for randomly oriented or aligned initial conditions, respectively. We identify three regimes: a high ψ , high ϕ moving order (MO) state for $D_{\theta} \leq 0.108$ in (a); a low ψ , high ϕ quenched disorder (QD) state for $0.125 < D_{\theta} \leq 0.32$ in (a) and $0.15 < R \leq 0.425$ in (c); and a low ψ , low ϕ dynamic disorder (DD) state for $D_{\theta} > 0.32$ in (a) and $R \leq 0.15$ or $R > 0.425$ in (c). Each point is averaged over the last 2×10^6 timesteps (of 2×10^7 total), after reaching the steady state. All simulations used the parameters detailed in the text.

for a sufficiently large R , the disks will be blocked from rotating by neighboring agents. This implies that the angular fluctuations generated by noise will be constrained by the interparticle repulsive forces. The tangential component of these forces corresponds to a restitution force that opposes the disks' angular fluctuations while their radial component becomes a retrograde force in the $-\hat{n}_i$ direction. We will show below that the angular dynamics are well described by an Ornstein-Uhlenbeck process [54] and that the transition from the MO phase to the QD phase will occur when the mean retrograde force matches self-propulsion.

We begin by writing an expression for the effective restitution force that results from the repulsion of neighboring disks. For small angular fluctuations $\Delta\theta(t)$, about the equilibrium point with $\Delta\theta(t) = 0$, the arc followed by the geometric center of the disk can be approximated by a linear displacement $\Delta x = R\Delta\theta$. In the packed case considered here, the agents will thus approximately feel, in average, a linear restitution force given by $\vec{f} \cdot \hat{n}^{\perp} \approx -(k/c)\Delta x$, where c is a proportionality constant that results from averaging over the multiple configurations of neighbor positions and angular fluctuations. If we then replace this expression into the angular equation

of motion (2), we find that, at first order in $\Delta x \ll 1$, the orientation dynamics reduces to an Ornstein-Uhlenbeck process [54] described by

$$\dot{\Delta\theta} = -\frac{\beta k R}{c} \Delta\theta + \sqrt{2D_\theta} \eta(t). \quad (3)$$

Here, $\eta(t)$ is a random variable that describes a noise with zero mean and variance $\langle \eta(t)\eta(t') \rangle = \delta(t-t')$. The mean-square fluctuation of the orientation as a function of time thus becomes

$$\langle \Delta\theta^2 \rangle(t) = \frac{cD_\theta}{\beta k R} \left(1 - e^{-2\beta k R t/c} \right). \quad (4)$$

Figure 3(a) confirms that, in the MO and the QD state, the mean-square fluctuations of the orientation as a function of time follow our analytical description. The symbols display the $\langle \Delta\theta^2 \rangle$ values obtained from numerical simulations; the curves correspond to plots of Eq. (4) with $c = 4$. The figure shows that both solutions match very well for the parameters considered in this paper (specified above) and three different D_θ noise levels. At short timescales, Eq. (4) shows that the angular fluctuations in the QD state follow a diffusive behavior with $\langle \Delta\theta^2 \rangle \simeq 2D_\theta t$. At long timescales, they saturate at a mean-square value

$$\langle \Delta\theta^2 \rangle_s = \frac{4D_\theta}{\beta k R}, \quad (5)$$

with characteristic crossover time $\tau \sim 4/\beta k R$.

Figure 3(b) compares the numerical $\langle \Delta\theta^2 \rangle_s$ values after reaching the steady state, as a function of D_θ for fixed $R = 0.3$ (\circ) and as a function of R for fixed $D_\theta = 0.15$ (\diamond), to the analytical expression in Eq. (5) vs. D_θ (solid lines) and vs. R (dashed lines). We find an excellent match for $\langle \Delta\theta^2 \rangle \lesssim 0.5$ but strong deviations for higher $\langle \Delta\theta^2 \rangle$, as expected given our small angle approximations.

Using the results above, we can determine the transition between the MO and QD phases analytically. We begin by noting that the repulsive forces that constrain angular fluctuations not only affect $\dot{\Delta\theta}$, but also have a component in the $-\hat{n}$ direction. Defining the mean heading of a disk as $\hat{y} = \langle \hat{n} \rangle$, we can use Eq. (1) to compute the mean force along \hat{y} as

$$\langle F_{\hat{y}} \rangle = v_0 \langle \hat{n} \cdot \hat{y} \rangle + \alpha \langle (\vec{f} \cdot \hat{n})(\hat{n} \cdot \hat{y}) \rangle. \quad (6)$$

Since $\vec{f} \cdot \hat{n} = -k\Delta x \sin(\Delta\theta)/4$ and $\hat{n} \cdot \hat{y} = \cos(\Delta\theta)$, we find that $\langle F_{\hat{y}} \rangle \approx v_0 - (2v_0 + \alpha k R) \langle \Delta\theta^2 \rangle_s / 4$ at leading order in Δx . Using Eq. (5), we thus obtain

$$\langle F_{\hat{y}} \rangle \approx v_0 - (2v_0 + \alpha k R) \frac{D_\theta}{\beta k R}. \quad (7)$$

This expression shows that increasing the angular noise D_θ leads to stronger retrograde forces, which will eventually surpass the self-propulsion term v_0 and produce backward motion. When this occurs, the collisions generate anti-alignment forces that result in the quenched

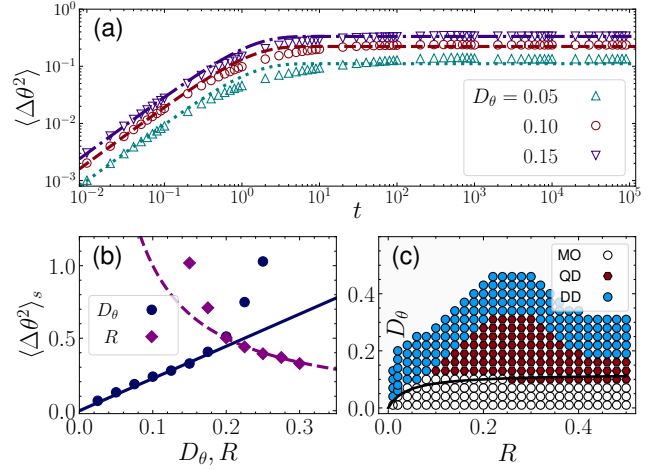


FIG. 3. (Color online) (a) mean-square orientation fluctuations $\langle \Delta\theta^2 \rangle$ as a function of time t , for $R = 0.3$ and three different values of D_θ . Numerical simulation results (symbols) are well matched by our analytical predictions (curves), expressed in Eq. (4), especially in the asymptotic regimes. (b) Stead-state mean-square orientation fluctuations as a function of angular noise D_θ and degree of rotational eccentricity R , for fixed $R = 0.3$ or fixed $D_\theta = 0.15$, respectively. The numerical simulations and analytical predictions expressed in Eq. (5) match well only for low $\langle \Delta\theta^2 \rangle$, as expected. (c) Phase diagram in the R - D_θ plane. The symbols indicate the phases obtained after reaching the steady state in simulations. No simulations were carried out in the region without symbols, where DD states are expected. The numerically obtained transition from moving order (MO) to quenched disorder (QD) is well matched by its analytical predictions (solid black curve), expressed in Eq. (8). All simulations used the parameters detailed in the text and randomly oriented initial conditions.

state. Hence, the critical noise D_θ^* can be computed by imposing $\langle F_{\hat{y}} \rangle = 0$ in Eq. (7), which yields

$$D_\theta^* = \frac{v_0 \beta k R}{2v_0 + \alpha k R}. \quad (8)$$

Figure 3(c) shows that the critical noise curve $D_\theta^*(R)$ matches very well the boundary between the different phases obtained numerically in the (R, D_θ) plane, for $v_0 = 0.002$ and all other parameter values specified above, thus validating our assumptions. The simulation results also show that QD emerges between the MO and DD phases for all $R \gtrsim 0.08$, and that there is an optimal $R \approx 2.26$ at which the QD state remains stable for the highest noise values. For $R \lesssim 0.08$, angular fluctuations are barely confined since the rotational dynamics are almost isotropic, so the QD mechanisms cannot develop.

In conclusion, our results demonstrate and explain the emergence of a novel, noise-induced QD phase that could be generically present in a broad range of dense active systems. Although we focused here in a limit case with only angular noise and no sideways displacements, our numerical explorations have shown that the

QD state also appears in simulations with a range of non-isotropic damping properties affecting the displacements and with positional noise in addition to the angular noise. We emphasize that this is the generally expected situation in real-world systems, where the polar nature of self-propelled agents can be expected to be reflected in anisotropic damping interaction with the substrate. Indeed, various experimental systems have analyzed agents with anisotropic damping [28, 32, 50, 55–57]. Furthermore, in addition to the general model introduced here, we also considered the presence of the QD phase for other models of active agents with repulsive interactions commonly used in the literature [39, 49, 58, 59], which are based on self-alignment towards the displacement direction rather than on mechanical torques. We find that QD also emerges (for a range of levels of anisotropy in the noise and the response to external forces) when the angular relaxation is nonlinear [49, 59], but not when it is linear [39, 58] (see Supplemental Material [53]). Consequently, we expect the QD state to emerge in experimental systems and encourage the design of setups that could detect it.

This work was supported by the National Natural Science Foundation of China, Grant 62176022, and by the John Templeton Foundation, Grant 62213. The work of Cristián Huepe was partially funded by CHuepe Labs Inc. The work of Guozheng Lin was partially funded by China Scholarship Council.

* gzhlin@mail.bnu.edu.cn

† zhan@mail.bnu.edu.cn

‡ amir.shee@northwestern.edu

§ cristian@northwestern.edu

- [1] P. Romanczuk, M. Bär, W. Ebeling, B. Lindner, and L. Schimansky-Geier, Active Brownian Particles, *Eur. Phys. J. Special Topics* **202**, 1 (2012).
- [2] J. Elgeti, R. G. Winkler, and G. Gompper, Physics of microswimmers: single particle motion and collective behavior: a review, *Reports on Progress in Physics* **78**, 056601 (2015).
- [3] C. Bechinger, R. Di Leonardo, H. Löwen, C. Reichhardt, G. Volpe, and G. Volpe, Active particles in complex and crowded environments, *Reviews of Modern Physics* **88**, 45006 (2016).
- [4] A. Doostmohammadi, J. Ignés-Mullol, J. M. Yeomans, and F. Sagués, Active nematics, *Nature Communications* **9**, 3246 (2018).
- [5] P. Guillamat, . Kos, J. Haroöün, J. Ignés-Mullol, M. Ravnik, and F. Sagués, Active nematic emulsions, *Science Advances* **4**, eaao1470 (2018).
- [6] A. Martín-Gómez, D. Levis, A. Díaz-Guilera, and I. Pagonabarraga, Collective motion of active Brownian particles with polar alignment, *Soft Matter* **14**, 2610 (2018).
- [7] I. Theurkauff, C. Cottin-Bizonne, J. Palacci, C. Ybert, and L. Bocquet, Dynamic Clustering in Active Colloidal Suspensions with Chemical Signaling, *Physical Review Letters* **108**, 268303 (2012).
- [8] J. Palacci, S. Sacanna, A. P. Steinberg, D. J. Pine, and P. M. Chaikin, Living Crystals of Light-Activated Colloidal Surfers, *Science* **339**, 936 (2013).
- [9] M. Paoluzzi, D. Levis, and I. Pagonabarraga, From motility-induced phase-separation to glassiness in dense active matter, *Communications Physics* **5**, 111 (2022).
- [10] Y. Fily and M. C. Marchetti, Athermal Phase Separation of Self-Propelled Particles with No Alignment, *Physical Review Letters* **108**, 235702 (2012).
- [11] T. Vicsek and A. Zafeiris, Collective motion, *Physics Reports* **517**, 71 (2012).
- [12] T. Speck, Collective behavior of active Brownian particles: From microscopic clustering to macroscopic phase separation, *The European Physical Journal Special Topics* **225**, 2287 (2016).
- [13] S. J. Kron and J. A. Spudich, Fluorescent actin filaments move on myosin fixed to a glass surface., *Proceedings of the National Academy of Sciences* **83**, 6272 (1986).
- [14] F. J. Ndlec, T. Surrey, A. C. Maggs, and S. Leibler, Self-organization of microtubules and motors, *Nature* **389**, 305 (1997).
- [15] V. Schaller, C. Weber, C. Semmrich, E. Frey, and A. R. Bausch, Polar patterns of driven filaments, *Nature* **467**, 73 (2010).
- [16] E. F. Keller and L. A. Segel, Model for chemotaxis, *Journal of Theoretical Biology* **30**, 225 (1971).
- [17] C. Dombrowski, L. Cisneros, S. Chatkaew, R. E. Goldstein, and J. O. Kessler, Self-Concentration and Large-Scale Coherence in Bacterial Dynamics, *Physical Review Letters* **93**, 098103 (2004).
- [18] H. P. Zhang, A. Beer, E.-L. Florin, and H. L. Swinney, Collective motion and density fluctuations in bacterial colonies, *Proceedings of the National Academy of Sciences* **107**, 13626 (2010).
- [19] J. Buhl, D. J. T. Sumpter, I. D. Couzin, J. J. Hale, E. Despland, E. R. Miller, and S. J. Simpson, From Disorder to Order in Marching Locusts, *Science* **312**, 1402 (2006).
- [20] S. Bazazi, P. Romanczuk, S. Thomas, L. Schimansky-Geier, J. J. Hale, G. A. Miller, G. A. Sword, S. J. Simpson, and I. D. Couzin, Nutritional state and collective motion: from individuals to mass migration, *Proceedings of the Royal Society B: Biological Sciences* **279**, 3376 (2012).
- [21] C. W. Reynolds, Flocks, Herds and Schools: A Distributed Behavioral Model, *SIGGRAPH Comput. Graph.* **21**, 25 (1987).
- [22] M. Nagy, Z. Ákos, D. Biro, and T. Vicsek, Hierarchical group dynamics in pigeon flocks, *Nature* **464**, 890 (2010).
- [23] B. L. Partridge, The effect of school size on the structure and dynamics of minnow schools, *Animal Behaviour* **28**, 68 (1980).
- [24] I. D. Couzin, J. Krause, R. James, G. D. Ruxton, and N. R. Franks, Collective Memory and Spatial Sorting in Animal Groups, *Journal of Theoretical Biology* **218**, 1 (2002).
- [25] J. E. Herbert-Read, A. Perna, R. P. Mann, T. M. Schaefer, D. J. T. Sumpter, and A. J. W. Ward, Inferring the rules of interaction of shoaling fish, *Proceedings of the National Academy of Sciences* **108**, 18726 (2011).
- [26] A. Bricard, J.-B. Caussin, N. Desreumaux, O. Dauchot, and D. Bartolo, Emergence of macroscopic directed motion in populations of motile colloids, *Nature* **503**, 95

- (2013).
- [27] A. Bricard, J.-B. Caussin, D. Das, C. Savoie, V. Chikkadi, K. Shitara, O. Chepizhko, F. Peruani, D. Saintillan, and D. Bartolo, Emergent vortices in populations of colloidal rollers, *Nature Communications* **6**, 7470 (2015).
- [28] J. Deseigne, O. Dauchot, and H. Chaté, Collective Motion of Vibrated Polar Disks, *Physical Review Letters* **105**, 098001 (2010).
- [29] J. Deseigne, S. Léonard, O. Dauchot, and H. Chaté, Vibrated polar disks: spontaneous motion, binary collisions, and collective dynamics, *Soft Matter* **8**, 5629 (2012).
- [30] H. Mori, Transport, Collective Motion, and Brownian Motion, *Progress of Theoretical Physics* **33**, 423 (1965).
- [31] A. E. Turgut, C. Huepe, H. Çelikkanat, F. Gökçe, and E. Şahin, Modeling Phase Transition in Self-organized Mobile Robot Flocks, in *Ant Colony Optimization and Swarm Intelligence*, edited by M. Dorigo, M. Birattari, C. Blum, M. Clerc, T. Stützle, and A. F. T. Winfield (Springer Berlin Heidelberg, Berlin, Heidelberg, 2008) pp. 108–119.
- [32] E. Ferrante, A. E. Turgut, C. Huepe, A. Stranieri, C. Pinciroli, and M. Dorigo, Self-organized flocking with a mobile robot swarm: a novel motion control method, *Adaptive Behavior* **20**, 460 (2012).
- [33] M. Brambilla, E. Ferrante, M. Birattari, and M. Dorigo, Swarm robotics: a review from the swarm engineering perspective, *Swarm Intelligence* **7**, 1 (2013).
- [34] S. Li, R. Batra, D. Brown, H.-D. Chang, N. Ranganathan, C. Hoberman, D. Rus, and H. Lipson, Particle robotics based on statistical mechanics of loosely coupled components, *Nature* **567**, 361 (2019).
- [35] K. H. Petersen, N. Napp, R. Stuart-Smith, D. Rus, and M. Kovac, A review of collective robotic construction, *Science Robotics* **4**, eaau8479 (2019).
- [36] M. Dorigo, G. Theraulaz, and V. Trianni, Reflections on the future of swarm robotics, *Science Robotics* **5**, eabe4385 (2020).
- [37] G. Oliveri, L. C. van Laake, C. Carissimo, C. Miette, and J. T. B. Overvelde, Continuous learning of emergent behavior in robotic matter, *Proceedings of the National Academy of Sciences* **118**, e2017015118 (2021).
- [38] T. Vicsek, A. Czirók, E. Ben-Jacob, I. Cohen, and O. Shochet, Novel Type of Phase Transition in a System of Self-Driven Particles, *Physical Review Letters* **75**, 1226 (1995).
- [39] B. Szabó, G. J. Szöllösi, B. Gönci, Z. Jurányi, D. Selmecki, and T. Vicsek, Phase transition in the collective migration of tissue cells: Experiment and model, *Physical Review E* **74**, 061908 (2006).
- [40] C. Huepe and M. Aldana, Intermittency and Clustering in a System of Self-Driven Particles, *Physical Review Letters* **92**, 168701 (2004).
- [41] F. Peruani, A. Deutsch, and M. Bär, Nonequilibrium clustering of self-propelled rods, *Physical Review E* **74**, 30904 (2006).
- [42] G. S. Redner, M. F. Hagan, and A. Baskaran, Structure and Dynamics of a Phase-Separating Active Colloidal Fluid, *Physical Review Letters* **110**, 055701 (2013).
- [43] M. E. Cates and J. Tailleur, When are active Brownian particles and run-and-tumble particles equivalent? Consequences for motility-induced phase separation, *EPL (Europhysics Letters)* **101**, 20010 (2013).
- [44] M. E. Cates and J. Tailleur, Motility-Induced Phase Separation, *Annual Review of Condensed Matter Physics* **6**, 219 (2015).
- [45] C. Reichhardt and C. J. O. Reichhardt, Active microrheology in active matter systems: Mobility, intermittency, and avalanches, *Physical Review E* **91**, 032313 (2015).
- [46] Y. Zhao, T. Ihle, Z. Han, C. Huepe, and P. Romanczuk, Phases and homogeneous ordered states in alignment-based self-propelled particle models, *Physical Review E* **104**, 44605 (2021).
- [47] Y. Zhao, C. Huepe, and P. Romanczuk, Contagion dynamics in self-organized systems of self-propelled agents, *Scientific Reports* **12**, 2588 (2022).
- [48] G. Lin, Z. Han, and C. Huepe, Orderdisorder transitions in a minimal model of active elasticity, *New Journal of Physics* **23**, 023019 (2021).
- [49] P. Baconnier, D. Shohat, C. H. López, C. Coulais, V. Démery, G. Düring, and O. Dauchot, Selective and collective actuation in active solids, *Nature Physics* **18**, 1234 (2022).
- [50] H. Xu, Y. Huang, R. Zhang, and Y. Wu, Autonomous waves and global motion modes in living active solids, *Nature Physics* **19**, 46 (2023).
- [51] S. Henkes, K. Kostanjevec, J. M. Collinson, R. Sknepnek, and E. Bertin, Dense active matter model of motion patterns in confluent cell monolayers, *Nature Communications* **11**, 1405 (2020).
- [52] S. Garcia, E. Hannezo, J. Elgeti, J.-F. Joanny, P. Silberzan, and N. S. Gov, Physics of active jamming during collective cellular motion in a monolayer, *Proceedings of the National Academy of Sciences* **112**, 15314 (2015).
- [53] See supplemental material at [publisher will insert url] for model derivation, analytic calculations, robustness, and comparison to other models.
- [54] I. Karatzas and S. E. Shreve, *Brownian Motion and Stochastic Calculus*, Vol. 113 (Springer New York, New York, NY, 1998) pp. XXIII–470.
- [55] Y. Zheng, C. Huepe, and Z. Han, Experimental capabilities and limitations of a position-based control algorithm for swarm robotics, *Adaptive Behavior* **30**, 19 (2020).
- [56] Z. Liu, A. E. Turgut, B. Lennox, and F. Arvin, Self-organised Flocking of Robotic Swarm in Cluttered Environments, in *Towards Autonomous Robotic Systems*, edited by C. Fox, J. Gao, A. Ghalamzan Esfahani, M. Saa, M. Hanheide, and S. Parsons (Springer International Publishing, Cham, 2021) pp. 126–135.
- [57] J. Qi, L. Bai, Y. Wei, H. Zhang, and Y. Xiao, Emergence of adaptation of collective behavior based on visual perception, *IEEE Internet of Things Journal* , 1 (2023).
- [58] S. Henkes, Y. Fily, and M. C. Marchetti, Active jamming: Self-propelled soft particles at high density, *Physical Review E* **84**, 040301 (2011).
- [59] O. Dauchot and V. Démery, Dynamics of a Self-Propelled Particle in a Harmonic Trap, *Physical Review Letters* **122**, 068002 (2019).